European Review for Medical and Pharmacological Sciences 2013; 17: 644-652

Decreased expression of p38 MAPK mediates protective effects of hydrogen sulfide on hepatic fibrosis

H.-N. FAN, H.-J. WANG, L. REN, B. REN, C.-R. Y. DAN, Y.-F. LI, L.-Z. HOU, Y. DENG

Department of Hepatopancreatobiliary Surgery, Affiliated Hospital of Qinghai University, Xining, Qinghai, P.R. China

Abstract. – AIM: To investigate the *in vitro* and *in vivo* effects of hydrogen sulfide (H_2S) on activated hepatic stellate cells (HSCs) and carbon tetrachloride (CCl_4)-induced hepatic fibrosis rats. To explore the *in vitro* and *in vivo* expression of Phospho-p38, Phospho-Akt and NF-kB in HSCs treated with H_2S.

MATERIALS AND METHODS: HSC-T6 cells were incubated and activated with 500 μg/L ferric nitrilotriacetate (Fe-NTA), and then were incubated with NaHS, an H_2S-releasing molecule for 6, 12, 24 and 48 h. MTT assay was performed to detect cell viability. Propidium iodide (PI) staining was used to determine cell cycle by flow cytometry. Apoptosis was detected with Annexin-V FITC (fluorescein isothiocyanate) and PI (propidium iodide) double staining. Western blotting was performed to detect protein expressions of Phospho-p38, Phospho-Akt and NF-kB. Hepatic fibrosis model was established by intraperitoneal injection of CCl_4 in male Wistar rats, and rats were randomly divided into three groups, including healthy control, rats treated with CCl_4 + saline, and rats treated with CCl_4 + NaHS. Immunohistochemistry analysis was performed to measure protein expression of Phospho-p38 and Phospho-Akt in rat hepatic samples.

RESULTS: NaHS inhibited the proliferation of Fe-NTA (nitrilotriacetic acid)-induced HSC-T6 cells in a dose-dependent way at 6, 12, 24 and 48 h. NaHS (500 μmol/L) induced G1 phase cell cycle arrest and promoted survival in Fe-NTA-induced HSC-T6 cells. NaHS decreased Phospho-p38 and increased Phospho-Akt expressions in Fe-NTA-induced HSC-T6 cells and CCl_4-induced liver fibrosis rats.

CONCLUSIONS: Exogenous H_2S inhibits activated HSC-T6 cells and induces cell cycle arrest and apoptosis. Decreased Phospho-p38 and increased Phospho-Akt expressions may mediate the anti-fibrosis effect by exogenous H_2S.

Key Words:

Hepatic fibrosis, Hydrogen sulfide, Hepatic stellate cells, p38, Akt, NF-kB.

Introduction

Hydrogen sulfide (H_2S) is the third category of gaseous molecules after nitric oxide and carbon monoxide with many physiological and pathological activities. In mammalian tissues, H_2S is endogenously produced by cystathionine c-lyase (CSE) and cystathionine b-synthase (CBS), and exists in the form of NaHS (2/3) and H_2S (1/3)[1]. H_2S demonstrates a variety of therapeutic activities, and has been reported to suppress the development of myocardial infarct[2], hypoxic pulmonary hypertension[3], neuronal injury[4] and hypertension[5]. Recently, H_2S has also been found to play a key role in the regulation of hepatic physiology and pathology[6]. In mammalian hepatic tissues, H_2S could activate ATP sensitive potassium (KATP) channels and result in vasorelaxation of the hepatic artery[7]. H_2S also has cytoprotective effects against hepatotoxicity, liver cirrhosis and portal hypertension in rats[8]. Hepatic fibrosis is the early phase of cirrhosis and its pathogenesis includes oxidative stress, inflammatory response and hepatotoxicity. Therefore, it is possible that H_2S have a protective effect against hepatic fibrosis.

Hepatic fibrosis is wound-healing response characterized by the accumulation of extracellular matrix (ECM) following hepatic diseases such as chronic hepatitis and liver damage. Hepatic stellate cells (HSCs) are the major cells in hepatic fibrosis and can be activated and transformed into fibrogenic myofibroblast-like cells, with enhanced proliferation, fibrogenesis and ECM synthesis[9]. Therefore, inhibiting the activation and proliferation of HSCs can be an attractive anti-fibrosis strategy.

This study aimed to investigate the protective effects of NaHS, an H_2S-releasing molecule, on *in vitro* activated HSCs and carbon tetrachloride

Corresponding Author: Yong Deng, MD; e-mail: dengyong@medmail.com.cn

(CCl_4)-induced hepatic fibrosis rats. We also detected the *in vitro* and *in vivo* expression of Phospho-p38 and Phospho-Akt in HSCs and rats treated with H_2S.

Materials and Methods

Cell Culture

HSC-T6 is a rat hepatic stellate cell line and was purchased from the Institute of Biochemistry and Cell Biology, Shanghai Institutes for Biological Sciences, Chinese Academy of Sciences. Cells were cultured with high glucose DMEM (Dulbecco's modified Eagle's medium) media (Invitrogen-GIBCO, Carlsbad, CA, USA), supplemented with 10% fetal bovine serum (FBS) (Sijichun Bioengineering Materials Inc., Hangzhou, Zhejiang, China), at 37°C in a humidified incubator with 5% CO_2. In order to fully activating HSCs, HSC-T6 cells were cultured for at least 2 week before subsequent experiments.

Cell Viability Assay

The MTT (Sigma Chemical Co., St. Louis, MO, U.S.A.) assay was performed to determine viable cells and cell growth. Briefly, cells at the logarithmic growth phase were seeded at a density of 1×10^3 cell/mL into 96-well culture plates, with 100 μL cell suspension in each well. Then cells were incubated with 500 μg/L of ferric nitrilotriacetate (Fe-NTA, Sigma, St. Louis, MO, USA) and (or) different concentrations of NaHS (Sigma, St. Louis, MO, USA) (0, 100, 200, 500 μmol/L). After treatment for 6, 12, 24 and 48 h, 10 μL of MTT solution (5 mg/mL) was added into each well and incubated at 37°C for 4 h, then centrifugation was performed at 3000 rpm for 10 minutes, and the supernatant was discarded to obtain the formazan pellet. Finally the pellet was dissolved completely with 100 μL DMSO. An ELISA plate reader was applied to measure the absorbance at 570 nm wavelength to determine the amount of pellet.

Cell Cycle Analysis

HSC-T6 cells at the logarithmic growth phase were seeded in 60-mm culture dishes. After reaching 50% confluence, the cells were cultured in serum-free medium for 24 h, and then were incubated with Fe-NTA (nitrilotriacetic acid) (500 μg/L) and (or) 500 μmol/L of NaHS for 48 h. The cells were harvested by trypsinization, and after PBS (phosphate buffered saline) washing, cells were resuspended in cold 70% ethanol. Finally, 1 propidium iodide (20 μg/ml) staining solution was added to the samples and associated data were analyzed on a FACScan (Becton Dickinson, San Francisco, CA, USA). Results were acquired from 10,000 cells.

Cell Apoptosis Assay

HSC-T6 were randomly divided into four groups: normal control group, NaHS group (500 μmol/L), Fe-NTA group (500 μg/L), and Fe-NTA + NaHS group. After incubation for 48 h, at least 2×10^5 cells were harvested from each group for apoptosis assay. After centrifugation at 2000 rpm for 5 minutes and PBS buffer washing, the pellet was resuspended in 100 μL 1×binding buffer, and 2.5 μL Annexin V and 5 μL PI (final concentration of 10 μg/mL) were added for incubation at room temperature in the dark. After 15 min, apoptosis was determined by flow cytometry and associated data were analyzed using Lysis software. At least 10,000 events were analyzed for each sample.

Western Blotting Analysis

HSC-T6 cells were cultured and treated with NaHS (500 μmol/L) and (or) Fe-NTA (500 μg/L) for 24 h. Proteins from HSC-T6 cells were extracted and their concentrations were determined by bicinchoninic acid protein concentration assay kit (Beijing Biosea Biotechnology Co. Ltd., China). The cell lysates (50 μg) were resolved by 15% sodium-dodecyl-sulfate-polyacrylamide gels (SDS-PAGE) and electrophoretically transferred to PVDF membrane, and then incubated with primary rabbit antibodies against Phospho-p38 or Phospho-Akt (Santa Cruz Biotechnology, Santa Cruz, CA, USA). The horseradish peroxidase-conjugated goat anti-rabbit second antibody was used at 1:1000 dilutions for 2 h at room temperature. Blots were visualized using the chemiluminescence method. β-actin was used as an internal control.

Animal Model of Hepatic Fibrosis

All studies were approved by the Animal Study Committee of the Qinghai University School of Medicine. Male Wistar rats (weighing 220-240 g) were supplied by the Animal Research Center at the Affiliated Hospital of Qinghai University. Rats were housed on standard laboratory rat chow on a 12-h light/dark cycle with temperature maintained at 22-23°C. Hepatic fibrosis was induced by CCl_4 injection. Briefly,

rats were administered phenobarbital sodium (0.35 g/L) with drinking water for 3 days, followed by intraperitoneal injection of CCl_4 (100 μL CCl_4/100 g body weight) in an equal volume of paraffin oil. These treatments were performed twice a week for 6 weeks. The control group received intraperitoneal injection of saline (100 μL saline/100 g body weight) in an equal volume of paraffin oil.

Animal Experiment

Twenty-four rats with hepatic fibrosis after receiving CCl_4 injections for 6 week were randomly divided into 2 groups (each had 12 rats): saline and NaHS, and received intraperitoneal injections of 1 ml of saline or NaHS solution (10 mmol/kg body weight), respectively, every two days for 6 weeks. Twelve rats in control group received intraperitoneal injections of 1 ml of saline for 6 weeks. After the experiments, the rats were sacrificed, and blood was collected via cardiac puncture, then the liver tissue was collected. Serum and liver samples were prepared and stored at 4°C.

Immunohistochemistry Analysis

Liver sections (5 mm in thickness) were incubated at 4°C overnight with primary antibody against Phospho-p38 or Phospho-Akt (Santa Cruz Biotechnology, Santa Cruz, CA, U.S.A) at the concentrations of 1:100. The horseradish peroxidase-conjugated secondary antibody (1:100) was used for 30 min at 37°C. After Tris Buffered Saline washing, sections were incubated with complex/horseradish peroxidase (1:200 dilution) for 30 min at 37°C. Sections were immersed in 0.05% 3,3'-diaminobenzidine tetrahydrochloride for immunolocalization. Slides were counterstained with hematoxylin before dehydration and mounting. Slides incubated with saline other than primary antibody served as a control for the background staining. In the vision field, the brown positive cells were counted as positive cells, and the total counts were converted into cell densities for quantitation.

Statistical Analysis

All quantitative data were expressed as mean ± standard deviation (SD). The commercially available software, SPSS version 14.0 (SPSS Inc., Chicago, IL, USA) was applied in statistical analysis. Student *t* test (unpaired, two tailed) was performed to compare the means between two groups. $p < 0.05$ was considered as statistically significant difference.

Results

H_2S Inhibited HSCs Activation Induced by Fe-NTA

To simulate the activated rat hepatic stellate cells model, HSC-T6 cells were incubated with Fe-NTA (500 μmol/L). Then these cells were simultaneously treated with various concentrations of NaHS (0, 100, 200, or 500 μmol/L) for different time points (6 h, 12 h, 24 h, 48 h). HSC-T6 cells treated with PBS served as normal control. The MTT assay revealed that Fe-NTA treatment could promote HSCs proliferation and increase viable cells in a time-dependent way, which was demonstrated with higher OD (optical density) values at 570 nm. However, NaHS inhibited cell viability in HSC-T6 treated with Fe-NTA in dose-dependent and time-dependent ways, and showed most potent effect in cell viability at 500 μmol/L concentration in all time points (Figure 1A). Therefore, we chose 500 μmol/L of NaHS in following experiments.

To investigate the detailed mechanism of the anti-proliferative activity of NaHS, cell cycle distribution was determined by flow cytometry. HSC-T6 cells were treated with NaHS (500 μmol/L) and (or) Fe-NTA (500 μg/L) for 48 h. NaHS increased the percentage of cells in the G1 phase significantly, while decrease percentage of cells in the S phase correspondingly ($p < 0.05$). However, the percentage of G2 cells remained unchanged after NaHS treatment (Figure 1B). This assay indicates that NaHS inhibited HSCs proliferation by inducing G1 phase arrest.

To investigate whether decreased viable cells was caused by increased apoptosis by NaHS treatement, HSC-T6 cells were cultivated in the presence of Fe-NTA and (or) NaHS for 48 h, and were double stained with Annexin V-FITC and PI. We found Fe-NTA increased the apoptotic rate of HSC-T6 cells significantly. However, NaHS treatment showed a protective effect and decreased the apoptotic rate in HSC-T6 cells treated with Fe-NTA ($p < 0.05$) (Figure 1C, D). NaHS treatment (500 μmol/L) alone did not increase apoptotic rate, which indicates the anti-apoptotic effect of NaHS may be related with oxidative stress induced by Fe-NTA.

H_2S Decreased Expression of Phosphorylated p38 MAPK and Increased Phospho-Akt in Fe-NTA activated HSCs

To investigate the involved apoptosis signaling pathways underlying NaHS treated HSC-

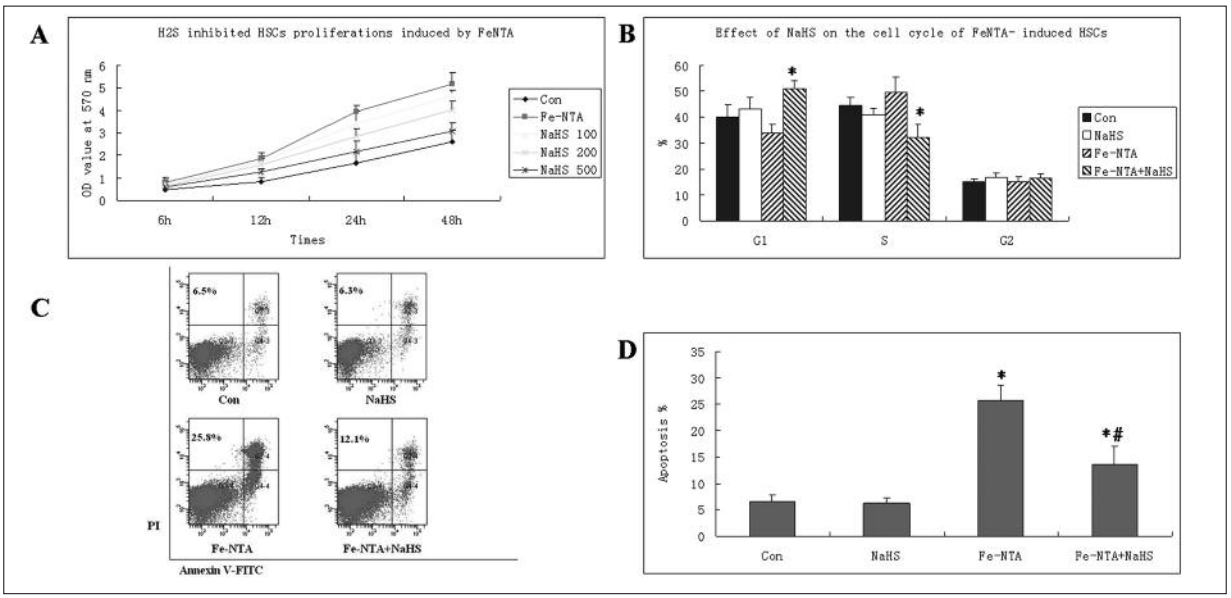

Figure 1. H_2S inhibited HSCs activation Fe-NTA-induced HSC-T6 cells. ***A,*** NaHS inhibited cell proliferation of Fe-NTA-induced HSC-T6 cells. Cells were seeded onto 96-well culture plates, incubated with Fe-NTA (500 μmol/L) and various concentrations of NaHS (0, 100, 200, or 500 μmol/L). After incubation for 6, 12, 24, 48 h, MTT assay was carried out to determine cell proliferation. The viable cells were represented with OD values at 570 nm. ***B,*** Cells were incubated with Fe-NTA (500 μmol/L) and (or) NaHS (500 μmol/L) for 48 h. Propidium iodide (PI, 20 μg/ml) staining was performed to determine the percentages of G1, S and G2 phases. Significant difference from the Fe-NTA group is denoted by ''*''. ***C,*** HSC-T6 cells were randomly divided into control, NaHS, Fe-NTA and Fe-NTA +NaHS group. Cell apoptosis was determined for Annexin-V FITC and PI double staining using flow cytometry at 48 h of treatment. NaHS treatment did not increase apoptotic rate in HSC-T6 cells. Fe-NTA increased the apoptosis rate significantly in HSC-T6 cells ($p < 0.05$), which could be attenuated by NaHS. Representative pictures from three experiments are shown. ***D,*** Apoptotic rates were shown in control, NaHS, Fe-NTA, Fe-NTA +NaHS group. Annexin V+/PI− and Annexin V+/PI+ populations were considered as apoptosis cells. Data were expressed as mean ± SD. A two-tailed, unpaired t-test was performed to compare the differences between two groups. Significant difference from the control group is denoted by ''*'' ($p < 0.05$). Significant difference from the Fe-NTA group is denoted by "#".

T6 cells, two signaling proteins associated with oxidative stress, such as Phospho-p38 MAPK and Phospho-Akt were investigated for their protein expression. HSC-T6 cells were randomly divided and treated with PBS, NaHS, Fe-NTA or Fe-NTA+NaHS for 48 h. Western blotting showed that Fe-NTA significantly increased Phospho-p38 and decreased Phospho-Akt protein expression. NaHS could significantly decrease the Phospho-p38 and increase Phospho-Akt protein levels in Fe-NTA treated HSC-T6 cells (Figure 2A).

To further investigate whether Phospho-p38 and Phospho-Akt participate in NaHS induced inhibition of HSCs activation induced by Fe-NTA, we treated HSC-T6 cells with NaHS or specific inhibitors of Phospho-p38 or Phospho-Akt in the presence of Fe-NTA treatment. The MTT assay revealed that SB203580 (inhibitors of Phospho-p38) and Perifosine (inhibitors of Phospho-Akt) both demonstrated proliferation inhibition effect on HSC-T6 cells treated with Fe-NTA. Moreover, these specific inhibitors also attenuated apoptosis induced by Fe-NTA (Figure 2B). The similar effects on cell proliferation and apoptosis in HSC-T6 cells between these inhibitors and NaHS indicates Phospho-p38 and Phospho-Akt may important mediators in protective effects of hydrogen sulfide on hepatic fibrosis.

To explore the interrelationships between Phospho-p38 and Phospho-Akt in Fe-NTA induced HSCs activation, HSC-T6 cells were treated with Fe-NTA, SB203580 or Perifosine for 48 h, and the protein expressions of Phospho-p38 and Phospho-Akt were detected. Western blotting showed that specific inhibitor of Phospho-p38 could significantly reduced the protein expression of Phospho-Akt induced by Fe-NTA, while Phospho-p38 protein expression remained unchanged in the presence of Perifosine. This indicates Phospho-p38 may be a mediator upstream of Phospho-Akt.

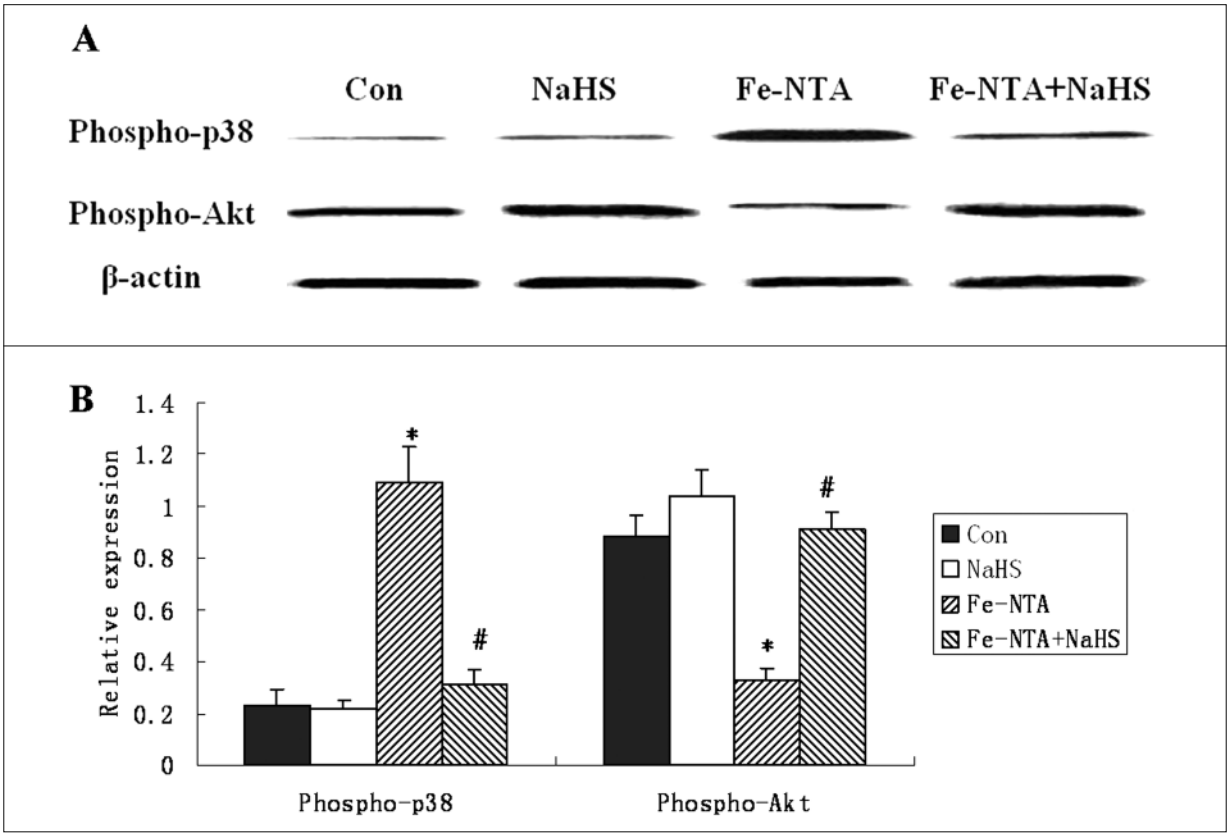

Figure 2. H_2S decreased expression of Phospho-p38 MAPK and increased Phospho-Akt in Fe-NTA activated HSCs. ***A,*** Protein expressions of Phospho-p38 MAPK and Phospho-Akt after NaHS treatment in Fe-NTA-activated HSC-T6 cells. HSC-T6 cells were treated with PBS (Control group), NaHS, Fe-NTA or Fe-NTA+NaHS for 48 h. Whole hepatic cell extracts were immunoblotted with the antibodies against Phospho-p38 and Phospho-Akt. ***B,*** The density of each band was converted into grayscale values and normalized to that of the internal control β-actin. Results are expressed as mean ± SD. Phospho-p38 and Phospho-Akt protein expressions were significantly higher in the Fe-NTA group compared with the normal group ($p < 0.05$), which was decreased by NaHS treatment. $^{*}p < 0.05$ vs control group; $^{\#}p < 0.05$ vs Fe-NTA group.

H_2S attenuates CCl_4-induced Lver Fibrosis and Decreased Phosphorylated p38 MAPK Expression

To confirm the protective effects of hydrogen sulfide on hepatic fibrosis, we established rat hepatic fibrosis model by receiving CCl_4 injections, and were randomly assigned into 2 groups, and were received saline and NaHS, respectively. Healthy rats receiving the same volume of saline served as normal control. There were almost no collagen fibers of blue color in HE-stained liver sections from healthy controls, however, abundant and widespread fibers of blue color were found in CCl_4-induced fibrosis rats injected with saline. This indicates that hepatic fibrosis model was successfully established (Data not shown).

We detected the *in vivo* expression of Phospho-p38 and Phospho-Akt in CCl_4-induced hepatic fibrosis rats. Immunohistochemistry analysis showed the Phospho-p38 protein expression was stronger in CCl_4 injection group than in control group, which could by lowered By NaHS treatment, which was in accordance with the results in Fe-NTA treated HSC-T6 cells. On the contrary, the expression of Phospho-Akt was lower in CCl_4 injection group than in control group, and was enhanced by NaHS treatment (Figure 4A). Quantification analysis showed NaHS decreased Phospho-p38 and increased Phospho-Akt protein significant in CCl_4-induced hepatic fibrosis rats ($p < 0.05$) (Figure 4B).

Discussion

In this study, we found NaHS, a bioactive compound releasing H_2S, showed protective effects on in vitro hepatic fibrosis model, demonstrated by suppressed cell proliferation, arrested cell cycle, and reduced apoptosis in Fe-NTA-

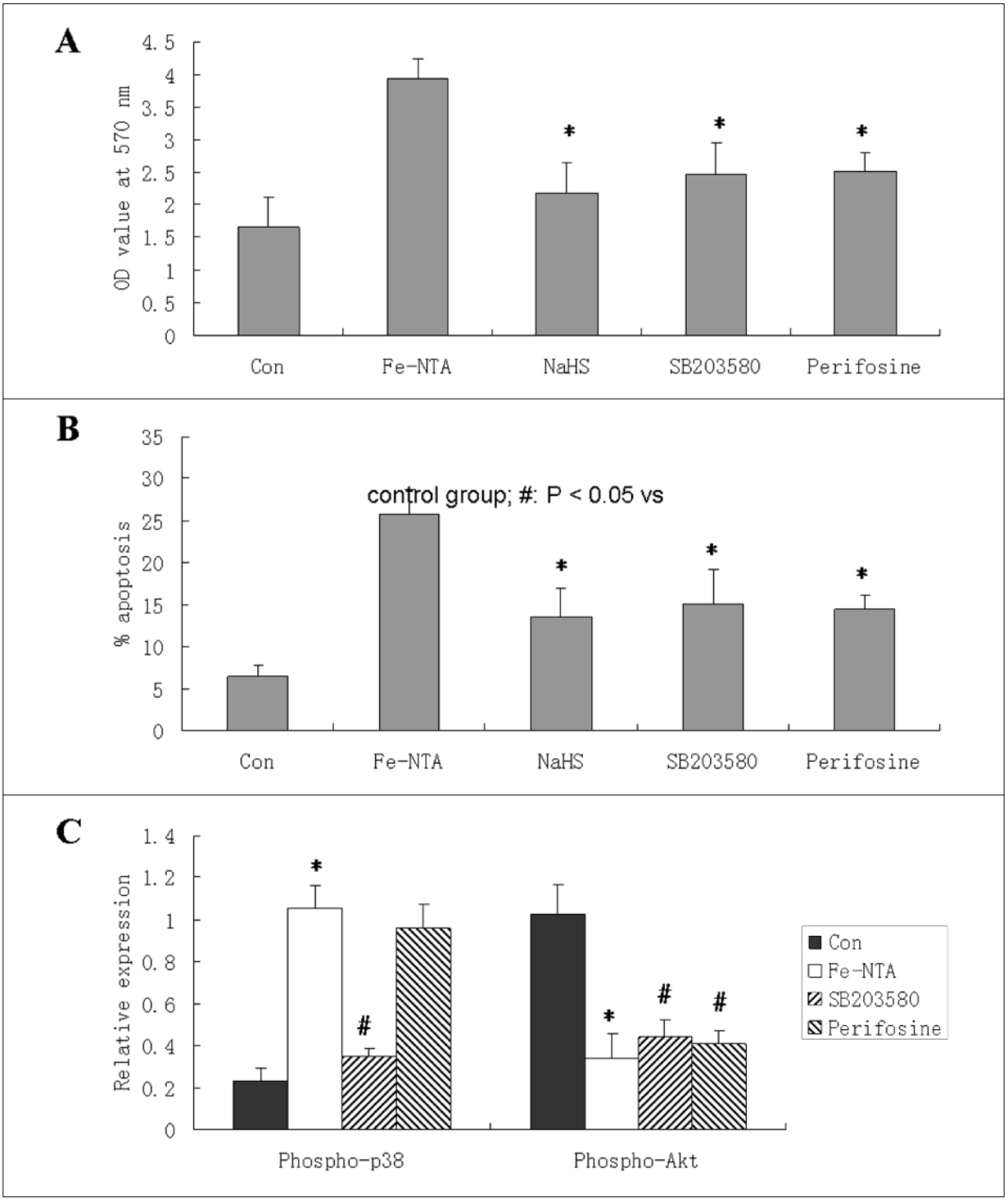

Figure 3. Phospho-p38 and Phospho-Akt participated in inhibitory effects of NaHS on Fe-NTA activated HSCs. ***A,*** Effects of inhibitors of Phospho-p38 and Phospho-Akt on cell proliferation in Fe-NTA-activated HSC-T6 cells. Cells were treated with PBS, Fe-NTA, Fe-NTA+NaHS, Fe-NTA+SB203580 (Inhibitor of p38), Fe-NTA+ Perifosine (Inhibitor of Akt) for 48 h. Cell proliferation was determined by MTT assay. ***B,*** Effects of inhibitors of Phospho-p38 and Phospho-Akt on apoptosis in Fe-NTA-activated HSC-T6 cells. Apoptosis was determined by Annexin-V FITC and PI double staining. $^{*}p < 0.05$ vs Fe-NTA group. ***C,*** Phospho-p38 lies upstream of Phospho-Akt. HSC-T6 cells were treated with PBS, Fe-NTA, Fe-NTA+SB203580 or Fe-NTA+Perifosine for 48 h, and were immunoblotted with the antibodies against Phospho-p38 and Phospho-Akt. The density of each band was converted into grayscale values and normalized to internal control β-actin. Results are expressed as mean±SD. $^{*}p < 0.05$ vs control group; $^{\#}p < 0.05$ vs Fe-NTA group.

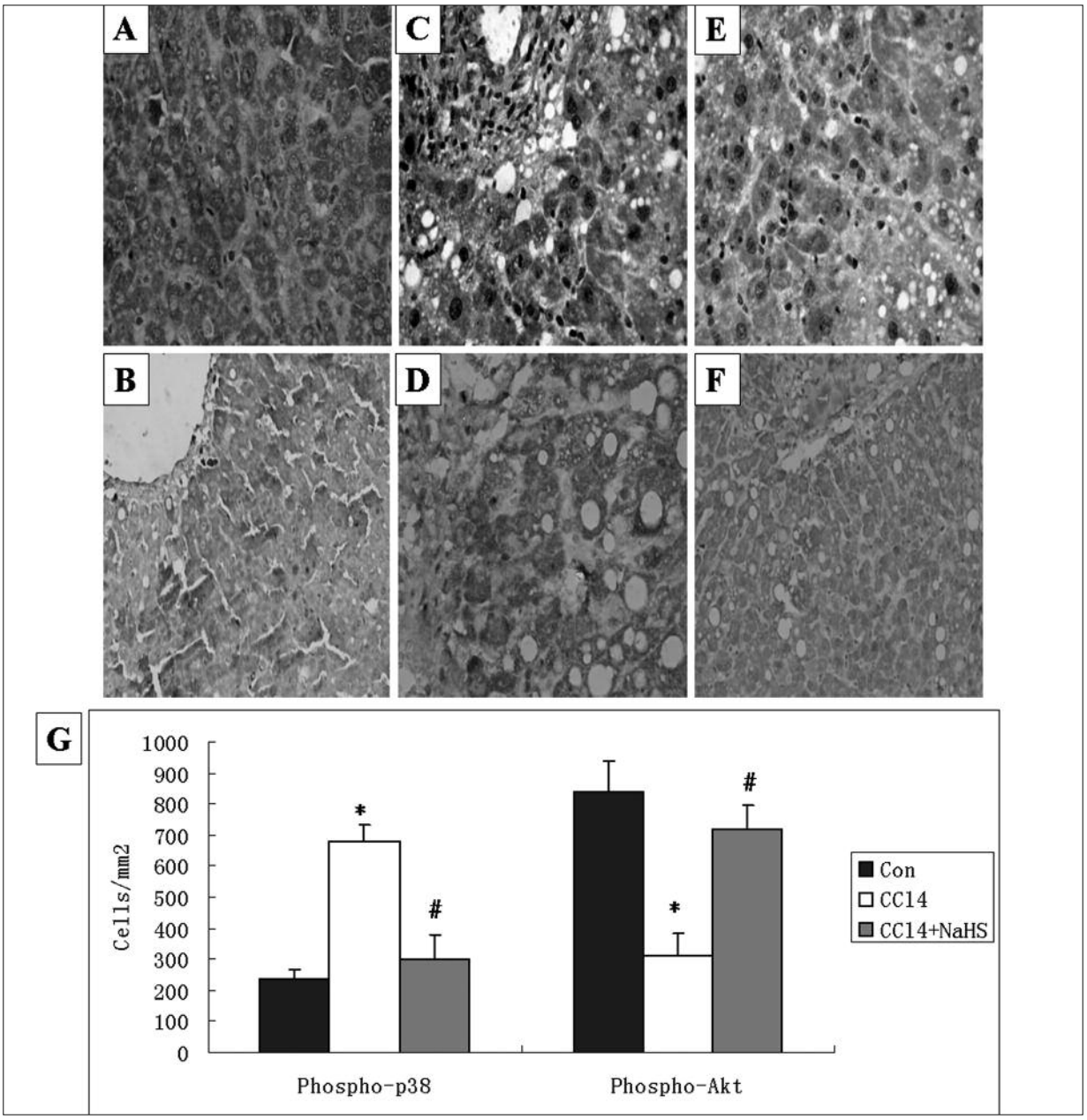

Figure 4. Immunohistochemistry analysis of Phospho-p38 and Phospho-Akt proteins in CCl_4 indueced hepatic fibrosis rats. Immunohistochemistry analysis of Phospho-p38 and Phospho-Akt proteins in hepatic sections from healthy controls ***(A, B)***, or rats treated with CCl_4 + saline ***(C, D)***, or CCl_4 + NaHS ***(E, F)***. Positive cells were labeled brown in the cytoplasm. Representative illustrations (400×magnification) of liver sections were shown. ***G,*** Quantification analysis showed significant increased Phospho-p38+ cells and decreased Phospho-Akt+ cells in the CCl_4-treated rats, compared with the healthy controls. In CCl_4-treated rats, the Phospho-Akt+ cells was decreased and Phospho-Akt+ cells were increased after NaHS treatment. Data were expressed as mean ± SD. *: a significant difference compared to the healthy controls. #: a significant difference compared to saline + CCl4-treated rats.

induced HSC-T6 cells. The underlying mechanisms may be related to decreased Phospho-p38 and increased Phospho-Akt expressions by NaHS treatment. The anti-fibrotic effects of NaHS were further confirmed in CCl_4-induced hepatic fibrosis rats with attenuated liver fibrosis and decreased Phospho-p38 and increased Phospho-Akt protein expression.

HSCs activation is the central pathogenesis in hepatic fibrosis, and inhibition of HSCs activa-

tion remains an important anti-fibrosis strategy. HSC-T6 is an immortalized rat liver stellate cell line with activated phenotype, and is often used as an *in vitro* research model for hepatic fibrosis[10]. In this study, we applied Fe-NTA in HSCs activation to establish *in vitro* hepatic fibrosis model. Fe-NTA produces hepatic parenchymal iron loading and free radical injury. In fact, iron deposition is common in hepatic fibrosis and can result in peroxidation of lipid membranes and oxidative stress, contributing to activation of HSCs and the development of hepatic fibrosis[11,12]. We found exogenous H_2S suppressed the proliferation of HSC cells dose-dependently. H_2S can decrease ROS generation and inhibit oxidative stress in cardiomyocytes under ischemia/reperfusion[13]. In our previous study, we also found NaHS decreased intracellular ROS level in Fe-NTA-activated HSC-T6 cells (Data not shown). This indicates the decreased proliferation of HSC-T6 cells may be associated with the antioxidant effect of NaHS. The hypothesis is further supported by the results that in HSCs with oxidative stress, Fe-NTA increased cell proliferation by elevating baseline intracellular pH (pHi) and Na+/H+ exchanger activity[14].

To explore the detailed mechanisms of decreased proliferation by NaHS treatment, we investigated the cell cycle and apoptosis of HSC-T6 cells. NaHS induced cell cycle arrest in the G1 phase, however, the apoptosis rate was reduced by NaHS in Fe-NTA-activated HSC-T6 cells, which contradicts the fact that the viable cells are reduced after NaHS treatment. It is possible that the effect of cell cycle arrest exceeds that of increased survived cells due to decreased apoptosis. In order to maintain the activated HSCs phenotype, apoptosis is inhibited in the molecular pathogenesis of hepatic fibrosis. Therefore, most anti-fibrosis agents exert their effects through pro-apoptotic activity on HSCs[15-17], and this pro-apoptotic activity is often was associated with increased intracellular oxidative stress in HSCs. Furthermore, apoptosis plays dual role in the development of hepatic fibrosis, and enhanced apoptosis is associated with worsening stages of fibrosis or regression of fibrosis, depending on the stage of fibrosis[18]. In early phase of hepatic fibrosis, oxidative stress is a major contributing factor to the activation and transformation of quiescent HSCs, leading to decreased antioxidant defense[19]. Therefore, NaHS may target the earth stage of hepatic fibrosis and inhibit apoptosis through antioxidant effect, while other agent may promote apoptosis through increased oxidative stress in the later stage, which deserves further investigation.

In order to explore the detailed mechanisms underlying protective effect of H_2S on HSCs activation, we measured the expression of two signal proteins which are associated with apoptosis and oxidative stress. NaHS decreased Phospho-p38 and increased Phospho-Akt proteins in Fe-NTA-activated HSCs and CCl_4-induced hepatic fibrosis rats. The phosphorylated p38 MAPK was inhibited by indole-3-carbinol in HSC-T6 cells, which was associated with decreaded HSCs proliferation and intracellular ROS[20]. Furthermore, inhibiting the p38 pathway could inhibit collagen synthesis and suppress liver fibrosis[21], which is in accordance with our results that SB203580, an inhibitor of p38, can inhibit proliferation and apoptosis in activated HSC-T6 cells. In our study, it is deserved to mention that the same concentrations of NaHS inhibit proliferation and apoptosis in Fe-NTA-activated HSC-T6 cells rather than untreated HSC-T6 cells. This can be explained by recent finding that ROS-induced p38-MAPK activation and apoptosis selectively effect on fibrogenic myofibroblast-like cells rather than on quiescent HSCs[22]. A constitutively active form of Akt has been reported to stimulate HSCs proliferation and collagen I expression[23]. In our study, however, NaHS-induced proliferation inhibition and survival are associated with increased phospho-Akt expression. NaHS increased Akt phosphorylation in interstitial cells of Cajal and hippocampal neurons[24,25]. Therefore, it is possible that H_2S exert its anti-apoptotic effects on activated HSCs through phospho-Akt.

Conclusions

NaHS shows protective effects on activated HSCs on in vitro and *in vivo* hepatic fibrosis models. Decreased Phospho-p38 and increased Phospho-Akt expressions may be the underlying mechanisms of NaHS. Our study suggests that exogenous H_2S is promising therapeutic strategy in treatment of hepatic fibrosis.

Acknowledgements

The study support by National Natural Science Foundation of China (NO: 30960374).

References

1) Renga B. Hydrogen sulfide generation in mammals: the molecular biology of cystathionine-β-synthase (CBS) and cystathionine-γ-lyase (CSE). Inflamm Allergy Drug Targets 2011; 10: 85-91.
2) Qipshidze N, Metreveli N, Mishra PK, Lominadze D, Tyagi SC. Hydrogen sulfide mitigates cardiac remodeling during myocardial infarction via improvement of angiogenesis. Int J Biol Sci 2012; 8: 430-441.
3) Olson KR, Whitfield NL, Bearden SE, St Leger J, Nilson E, Gao Y, Madden JA. Hypoxic pulmonary vasodilation: a paradigm shift with a hydrogen sulfide mechanism. Am J Physiol Regul Integr Comp Physiol 2010; 298: R51-60.
4) Zhang LM, Jiang CX, Liu DW. Hydrogen sulfide attenuates neuronal injury induced by vascular dementia via inhibiting apoptosis in rats. Neurochem Res 2009; 34: 1984-1992.
5) Ahmad FU, Sattar MA, Rathore HA, Abdullah MH, Tan S, Abdullah NA, Johns EJ. Exogenous hydrogen sulfide (H_2S) reduces blood pressure and prevents the progression of diabetic nephropathy in spontaneously hypertensive rats. Ren Fail 2012; 34: 203-210.
6) Fiorucci S, Distrutti E, Cirino G, Wallace JL. The emerging roles of hydrogen sulfide in the gastrointestinal tract andliver. Gastroenterology 2006; 131: 259-271.
7) Siebert N, Cantré D, Eipel C, Vollmar B. H_2S contributes to the hepatic arterial buffer response and mediatesvasorelaxation of the hepatic artery via activation of K (ATP) channels. Am J Physiol Gastrointest Liver Physiol 2008; 295: G1266-1273.
8) Tan G, Pan S, Li J, Dong X, Kang K, Zhao M, Jiang X, Kanwar JR, Qiao H, Jiang H, Sun X. Hydrogen sulfide attenuates carbon tetrachloride-induced hepatotoxicity, liver cirrhosis and portal hypertension in rats. PLoS One 2011; 6: e25943.
9) Tarrats N, Moles A, Morales A, García-Ruiz C, Fernández-Checa JC, Marí M. Critical role of tumor necrosis factor receptor 1, but not 2, in hepaticstellate cell proliferation, extracellular matrix remodeling, and liver fibrogenesis. Hepatology 2011; 54: 319-327.
10) Vogel S, Piantedosi R, Frank J, Lalazar A, Rockey DC, Friedman SL, Blaner WS. An immortalized rat liver stellate cell line (HSC-T6): a new cell model for the study of retinoid metabolism *in vitro*. J Lipid Res 2000; 41: 882-893.
11) Guo L, Enzan H, Hayashi Y, Miyazaki E, Jin Y, Toi M, Kuroda N, Hiroi M. Increased iron deposition in rat liver fibrosis induced by a high-dose injection of dimethylnitrosamine. Exp Mol Pathol 2006; 81: 255-261.
12) Ramm GA, Ruddell RG. Iron homeostasis, hepatocellular injury, and fibrogenesis in hemochromatosis: the role of inflammation in a noninflammatory liver disease. Semin Liver Dis 2010; 30: 271-287.
13) Sun WH, Liu F, Chen Y, Zhu YC. Hydrogen sulfide decreases the levels of ROS by inhibiting mitochondrial complex IV and increasing SOD activities in cardiomyocytes under ischemia/reperfusion. Biochem Biophys Res Commun 2012; 421: 164-169.
14) Svegliati Baroni G, D'Ambrosio L, Ferretti G, Casini A, Di Sario A, Salzano R, Ridolfi F, Saccomanno S, Jezequel AM, Benedetti A. Fibrogenic effect of oxidative stress on rat hepatic stellate cells. Hepatology 1998; 27: 720-726.
15) Tao LL, Cheng YY, Ding D, Mei S, Xu JW, Yu J, Ou-Yang Q, Deng L, Chen Q, Li QQ, Xu ZD, Liu XP. C/EBP-α ameliorates CCl(4)-induced liver fibrosis in mice through promoting apoptosis of hepatic stellate cells with little apoptotic effect on hepatocytes *in vitro* and *in vivo*. Apoptosis 2012; 17: 492-502.
16) Li CC, Yang CZ, Li XM, Zhao XM, Zou Y, Fan L, Zhou L, Liu JC, Niu YC. Hydroxysafflor yellow A induces apoptosis in activated hepatic stellate cells through ERK1/2 pathway *in vitro*. Eur J Pharm Sci 2012; 46: 397-404.
17) Kim IH, Kim SW, Kim SH, Lee SO, Lee ST, Kim DG, Lee MJ, Park WH. Parthenolide-induced apoptosis of hepatic stellate cells and anti-fibrotic effects in an *in vivo* rat model. Exp Mol Med 2012; 44: 448-456.
18) Chakraborty JB, Oakley F, Walsh MJ. Mechanisms and biomarkers of apoptosis in liver disease and fibrosis. Int J Hepatol 2012; 2012: 648915.
19) Mormone E, George J, Nieto N. Molecular pathogenesis of hepatic fibrosis and current therapeutic approaches. Chem Biol Interact 2011; 193: 225-231.
20) Ping J, Li JT, Liao ZX, Shang L, Wang H. Indole-3-carbinol inhibits hepatic stellate cells proliferation by blocking NADPH oxidase/reactive oxygen species/p38 MAPK pathway. Eur J Pharmacol 2011; 650: 656-662.
21) Zhang Y, Yao X. Role of c-Jun N-terminal kinase and p38/activation protein-1 in interleukin-1β-mediated type I collagen synthesis in rat hepatic stellate cells. APMIS 2012; 120: 101-107.
22) Jameel NM, Thirunavukkarasu C, Wu T, Watkins SC, Friedman SL, Gandhi CR. p38-MAPK- and caspase-3-mediated superoxide-induced apoptosis of rat hepatic stellate cells: reversal by retinoic acid. J Cell Physiol 2009; 218: 157-166.
23) Reif S, Lang A, Lindquist JN, Yata Y, Gabele E, Scanga A, Brenner DA, Rippe RA. The role of focal adhesion kinase-phosphatidylinositol 3-kinase-aktsignaling in hepatic stellate cell proliferation and type I collagen expression. J Biol Chem 2003; 278: 8083-8090.
24) Huang Y, Li F, Tong W, Zhang A, He Y, Fu T, Liu B. Hydrogen sulfide, a gaseous transmitter, stimulates proliferation of interstitial cells of Cajal via phosphorylation of AKT protein kinase. Tohoku J Exp Med 2010; 221: 125-132.
25) hao JL, Wan XH, Chen Y, Bi C, Chen HM, Zhong Y, Heng XH, Qian JQS. H_2S protects hippocampal neurons from anoxia-reoxygenation through cAMP-mediated PI3K/Akt/p70S6K cell-survival signaling pathways. J Mol Neurosci 2011; 43: 453-460.